CRISPR-Cas9 modified bacteriophage for treatment of *Staphylococcus aureus* induced osteomyelitis and soft tissue infection

Leah K. Horstemeyer, [1] JooYoun Park,[2] Elizabeth A. Swanson,[3] Mary Catherine Beard, [1] Emily M. McCabe, [1] Anna S. Rourke,[1] Keun Seok Seo,[2] Alicia K. Olivier,[4] Lauren B. Priddy[1]*

[1]Department of Agricultural and Biological Engineering, Mississippi State University, Mississippi State, MS, USA

[2]Department of Basic Sciences, College of Veterinary Medicine, Mississippi State University, Mississippi State, MS, USA

[3]Department of Clinical Sciences, College of Veterinary Medicine, Mississippi State University, Mississippi State, MS, USA

[4]Department of Pathobiology and Population Medicine, College of Veterinary Medicine, Mississippi State University, Mississippi State, MS, USA

*corresponding author

Contact: lbpriddy@abe.msstate.edu, (662) 325-5988, Department of Agricultural and Biological Engineering, Mississippi State University, 130 Creelman Street, Mississippi State, MS, USA 39762

Abstract

Osteomyelitis, or bone infection, is often induced by antibiotic resistant *Staphylococcus aureus* strains of bacteria. Although debridement and long-term administration of antibiotics are the gold standard for osteomyelitis treatment, the increase in prevalence of antibiotic resistant bacterial strains limits the ability of clinicians to effectively treat infection. Bacteriophages (phages), viruses that effectively lyse bacteria, have gained recent attention for their high specificity, non-toxicity, and the low likelihood of resistance development by pathogens. Previously, we have shown that CRISPR-Cas9 genomic editing techniques could be utilized to expand bacteriophage host range and enhance bactericidal activity through modification of the tail fiber protein, as well as improve safety with removal of major virulence genes. In a dermal infection study, these CRISPR-Cas9 phages reduced bacterial load relative to unmodified phage. Thus, we hypothesized this bacteriophage would be effective to mitigate infection from a biofilm forming *S. aureus* strain *in vitro* and *in vivo*. *In vitro*, qualitative fluorescent imaging demonstrated superiority of phage to conventional vancomycin and fosfomycin antibiotics against *S. aureus* biofilm. Quantitative antibiofilm effects increased over time for fosfomycin, phage, and fosfomycin-phage (dual) therapeutics delivered via alginate hydrogel. We developed an *in vivo* rat model of osteomyelitis and soft tissue infection that was reproducible and challenging and enabled longitudinal monitoring of infection progression. Using this model, phage (with and without fosfomycin) delivered via alginate hydrogel were successful in reducing soft tissue infection but not bone infection, based on bacteriological, histological, and scanning electron microscopy analyses. Notably, the efficacy of phage at mitigating soft tissue infection was equal to that of high dose fosfomycin. Future research may

50 utilize this model as a platform for evaluation of therapeutic type and dose, and alternate delivery
51 vehicles for osteomyelitis mitigation.

52 # Introduction

53 For nearly a century, antibiotics have been a vital resource utilized by clinicians to
54 eliminate infection, with nearly 270 million prescriptions dispensed in 2015 alone.[1] Antibiotics
55 are utilized for a variety of infections, from common otitis externa ("swimmers ear") to severe
56 endocarditis, pneumonia, meningitis or osteomyelitis. Although antibiotics are typically able to
57 clear infection, antibiotic resistant strains of bacteria continue to emerge. It is not as lucrative,
58 nor as feasible, for pharmaceutical companies to develop novel antibiotics at the rates that these
59 multi-drug resistant (MDR) bacterial strains are isolated. Nationally, approximately $2.2 billion
60 is spent annually to treat MDR bacterial infections.[2] By 2050, it is estimated that nearly 10
61 million people could die each year due to resistant strains of bacteria.[3]

62 *Staphylococcus aureus* (*S. aureus*), a gram-positive bacterial strain, is one of the most
63 commonly isolated and arguably one of the most detrimental pathogens with antibiotic
64 resistance. One of the most common antibiotic resistant strains of *S. aureus* is methicillin-
65 resistant *S. aureus* (MRSA). MRSA alone was responsible for over 80,000 reported infections in
66 2011 alone, of which 11,285 resulted in death.[4] *S. aureus* is able to achieve antibiotic
67 resistance with genomic changes such as altered synthesis of peptidoglycan, a major component
68 of the bacterial cell wall. Additionally, some strains of *S. aureus* can produce biofilms, an
69 extracellular polymeric matrix including dead bacterial cells, which surrounds and protects the
70 living, underlying layer of *S. aureus.*[5] These biofilms can be difficult to penetrate, and
71 oftentimes require surgical intervention to remove.

72 Difficulties in treating osteomyelitis, or the infection of bone, have been exacerbated by
73 the rise of antibiotic resistant bacterial strains, particularly *S. aureus* strains, which are the most
74 common cause of bone infection.[6] Of diabetic foot ulcers, which occur in 25% of diabetic
75 patients, approximately 20% will spread to nearby bony hosts and result in osteomyelitis.[7] As
76 diabetic diagnoses continue to increase in the United States with an expected 55 million to be
77 afflicted by 2030, osteomyelitis infections will be an ongoing challenge for the healthcare
78 community.[8] It is essential that new therapeutics be engineered and tested, for rapid translation
79 into clinical use.

80 Bacteriophages (phages), or viruses that kill their bacterial hosts, are one class of
81 therapeutics that have gained attention in recent years due to their high specificity, non-toxicity,
82 and abundancy in nature.[9,10] Phages have been used for decades in Eastern Europe but have
83 not yet been adopted in the United States or other countries. This may be due to public concern
84 regarding elective viral use, issues concerning commercial phage production, and/or the ability to
85 fund and validate clinical trials.[11] Nonetheless, the potential benefits of this treatment have
86 been indicated by results of clinical trials of phages for treating diabetic foot ulcers, chronic
87 otitis, and urinary tract infections[11–13]. In April 2019, data from clinical trials were published
88 from Sydney, Australia, where intravenous (IV) administration of phage was utilized for
89 *Staphylococcus* infection treatment. Marked reduction of *staphylococci* with no adverse events
90 were reported.[14] In the United States as of January 2019, IV administration of phage for
91 ventricular assist device infection treatment received approval for phase I/II clinical trials.[15]
92 Collectively, these clinical trials demonstrate the efficacy of bacteriophage therapeutics and
93 suggest their potential utility against MDR bacterial strains.

94 Hydrogels are a commonly used, easily tailored delivery vehicle for therapeutics for a
95 wide variety of ailments, including osteomyelitis[6,16,17]. Alginate hydrogels are injectable,
96 well characterized, and biocompatible.[18,19] Furthermore, bacteriophages have been
97 successfully delivered to sites of infection with various hydrogel-based delivery systems in
98 previous studies.[16,17,20]

99 Although the high specificity of phages can be beneficial for treating a known, single
100 species, specificity of these viruses can make polymicrobial infection mitigation challenging. In
101 the clinical scenario, it is ideal for health care providers to administer one broad-spectrum drug
102 immediately upon patient presentation, rather than spend time identifying the causative agents of
103 infection. Previously, we have utilized CRISPR-Cas9 to modify temperate bacteriophage, which
104 effectively removed major virulence genes and expanded host range via modifications to the tail
105 fiber protein (which codes host specificity). *In vitro* testing revealed the improvements of
106 bacteriophage bactericidal activity due to this CRISPR-Cas9 system.[21]Within 6h of treatment,
107 the CRISPR-Cas9 phage effectively killed $1x10^5$ CFU *S. aureus* culture. With native,
108 unmodified phage treatment, the culture was found to increase to approximately $1x10^9$ CFU.
109 Similar effects were noted in an *in vivo* dermal infection study, where CRISPR-Cas9 phage
110 treatment resulted in nearly complete mitigation of dermal infections (~1 log CFU/g tissue),
111 while treatment with unmodified phage resulted in a significantly higher bacterial load (~3.5 log
112 CFU/g tissue).[21]

113 The objectives of the present work were: (i) to develop a green fluorescent protein (GFP)
114 integrated *S. aureus* strain (ATCC 6538-GFP), modify bacteriophage using CRISPR-Cas9, and
115 evaluate the bactericidal efficacy of our CRISPR-Cas9 modified bacteriophage *in vitro*,
116 compared to conventional antibiotics, and (ii) to develop an *in vivo* model of osteomyelitis and

117 soft tissue infection using this biofilm forming *S. aureus* strain, and use it to assess the
118 antimicrobial effects of bacteriophage, antibiotic, and dual bacteriophage-antibiotic therapies via
119 histological, radiographic, and bacteriological analyses. Our hypothesis was that CRISPR-Cas9
120 modified bacteriophage would be effective against *S. aureus* infection *in vitro* and in the femur
121 and contiguous soft tissue *in vivo*.
122

123 Materials and Methods

124 Bacterial strains and culture

125 For a stable quantification of biofilm, *S. aureus* strain ATCC 6538 was genetically
126 modified to contain chromosomally integrated green fluorescent protein (GFP), as previously
127 described.[22] Briefly, *S. aureus* strain ATCC 6538 was transduced with a temperature sensitive
128 plasmid pTH100 harboring the GFP gene by electroporation and cultured in a brain heart
129 infusion (BHI) agar plate supplemented with chloramphenicol (BHI-CM) at 30°C, a plasmid
130 replication permissive temperature. To promote the first homologous recombination and cure
131 pTH100, a single colony grown in a BHI-CM plate was transferred to a fresh BHI-CM plate and
132 cultured at 42°C, a plasmid replication non-permissive temperature. To promote the second
133 homologous recombination, which removed the plasmid and resulted in a loss of
134 chloramphenicol resistance but maintained the GFP phenotype, a single colony was inoculated
135 into BHI broth and cultured at 37°C overnight. A serial dilution of culture was inoculated onto a
136 BHI plate and incubated at 37°C overnight. A GFP positive single colony checked by ultraviolet
137 lamp was randomly selected and streaked onto BHI and BHI-CM. A colony that was both GFP
138 positive and sensitive to chloramphenicol, indicating the integration of the GFP gene into the
139 chromosome and removal of plasmid, was selected for experiments (ATCC 6538-GFP).

140 ## Preparation of alginate hydrogels

141 All alginate gels were initially prepared at a 3% (w/v) concentration, for ultimate dilution
142 to 2% after loading them with therapeutic. A 3% alginate mixture (w/v) was made with alginic
143 acid powder (Sigma-Aldrich) and alpha Minimum Essential Medium (αMEM, Gibco) then left
144 overnight at room temperature. This solution was sterile filtered (0.2 μm, Pall) and transferred
145 into 1mL syringes. Therapeutics were then added directly to the alginate. The crosslinker,
146 calcium sulfate (0.21g $CaSO_4$ / mL distilled H_2O) was loaded into a separate 1mL syringe and
147 was mixed vigorously with the alginate solution for approximately one minute. Hydrogels were
148 kept at 4°C or on ice until use.

149 ## Synthesis of CRISPR-Cas9 modified bacteriophages

150 *S. aureus* strain RF122 harboring CRISPR-Cas9 modified bacteriophage was cultured in
151 BHI broth to the mid-exponential phase (OD600 at 0.3).[21] To induce CRISPR-Cas9 modified
152 bacteriophage, mitomycin C (1 μg/mL, Sigma-Aldrich) was added to the culture and further
153 incubated at 30°C with shaking at 80 RPM. A complete lysis of culture typically occurred within
154 2-3 hours. The clear lysate was sterilized with syringe filers (0.22 μm, Nalgene). The
155 concentration of phage was calculated by determining the plaque-forming units using a soft agar
156 (0.5%, w/v) overlaying method.[21]

157 ## Kirby-Bauer analyses

158 To analyze the bactericidal activity of therapeutics, a Kirby-Bauer assay was performed
159 as previously described, with slight modifications.[23] Stock solutions of fosfomycin (50
160 mg/mL) and phage (~10MOI/mL) were prepared in phosphate buffered saline (PBS). Using
161 these stock solutions, a total of 10μL of: (i) fosfomycin, (ii) phage, (iii) dual: fosfomycin (5μL)
162 and phage (5 μL), or (iv) PBS alone were directly applied to bacterial lawns, without the use of

163 disks as traditionally described. The applied solutions were allowed to set undisturbed for
164 approximately 5-10 minutes at room temperature, and were then incubated at 37°C for 24h. The
165 zones of inhibition were then measured and recorded.

166 Qualitative and quantitative bactericidal activity on biofilms

167 For qualitative *in vitro* evaluation of antibiofilm efficacy, a 6-well tissue culture plate was
168 pre-coated with 2% human serum for 24 hours, after which *Staphylococcus aureus* ATCC 6538-
169 GFP was cultured in tryptic soy broth (TSB) supplemented with 2% glucose for 72 hours. After
170 gentle washing with PBS, TSB supplemented with vancomycin (256, 512, or 1024 µg/mL),
171 fosfomycin (16, 64, 128 µg/mL) or bacteriophage (5, 10, or 25 multiplicity of infection (MOI))
172 was added to the biofilm and incubated for 24 hours. After gentle washing with PBS three times,
173 remaining biofilm indicated by GFP signal was measured using Cytation 5 plate reader (BioTek).
174 To quantify the antibiofilm activity of selected therapeutics delivered by alginate
175 hydrogels, fosfomycin, phage, or dual therapeutic was loaded in 2% alginate hydrogel and
176 overlaid on top of the biofilms. As a control, empty 2% alginate hydrogel was used. BHI broth
177 was added and cultures were incubated at 37°C for 24 h. After removing BHI broth, the entire
178 2% alginate hydrogel and biofilm were harvested and vigorously washed with PBS by
179 centrifugation to remove residual therapeutic. A serial dilution in PBS was plated onto BHI
180 plates to determine viable bacterial counts.

181 Rat osteomyelitis model

182 All procedures (Fig. 1) were performed in accordance with the Institutional Animal Care
183 and Use Committee (IACUC) of Mississippi State University. Charles River Sprague Dawley
184 female rats, 13 weeks old, were housed with 12h light/dark cycles and were provided food and
185 water *ad libitum.* Rats were administered slow release buprenorphine (1.0-1.2 mg/kg BW,

186 ZooPharm) pre-operatively for pain relief. Rats were anesthetized with isoflurane at an initial
187 concentration of 2-3%, and maintained at 1-2%. After sterile preparation of the left hindlimb by
188 fur removal and alcohol and chlorhexidine scrubs, the skin was incised with an anterior
189 approach, from the level of mid-diaphysis to the patella, along the lower half of the femur. The
190 muscle tissue was separated using blunt dissection along the muscle bundle divisions on the
191 anterolateral side of the femur. In the mid-diaphysis, a 1.2 mm (diameter) bicortical defect was
192 created with a pneumatic drill (Conmed Hall), and a #65 drill bit (McMaster-Carr). To mimic
193 contamination of orthopedic screws with *S. aureus* occurring in development of osteomyelitis *in*
194 *vivo,* sterile orthopedic screws (Antrin Miniature Specialties, #00-90) were placed into 200 μL of
195 a bacterial suspension (~$1x10^8$ CFU) of ATCC 6538-GFP for approximately 5-10 minutes
196 (average 6.5 min). The screw was then placed into a 96-well plate to dry for up to 6 minutes
197 (average 4 min). The bacterial load of these contaminated screws was approximately $5x10^4$ CFU,
198 determined by placing screws into 1mL of PBS, vigorously vortexing to elute bacteria from the
199 screw, then serially diluting the eluents for bacterial counting on BHI agar plates. *In vitro*
200 characterization of bacterial load based on (i) the time screws remained in culture (soak time)
201 and (ii) dry time was performed using the same procedure as for bacterial counts from *ex vivo*
202 screws. To assess the effect of soak time, dry time was kept at a constant 5 minutes, and
203 similarly for the effect of dry time, soak time was kept constant at 5 minutes. To complete the *in*
204 *vivo* procedure, the superficial fascia lata and skin were closed with sutures. Longitudinal
205 monitoring of infection at days 1, 3, and 6 post-infection was performed via radiographs with
206 fluorescent overlays using the IVIS Lumina XRMS II system (PerkinElmer).
207 After a 7 day infection period, the area was accessed along the original incision line. The
208 infected screw was removed and placed into 1mL PBS or fixative for bacterial counting or SEM,

209 respectively. Then, 100 µL of fosfomycin (3 mg), phage (MOI 3), dual (3 mg fosfomycin and
210 MOI 3 phage), or PBS loaded into 2% alginate hydrogel was injected into the lateral end of the
211 bicortical defect, with excess hydrogel pooling in the medial, underlying soft tissue.

212 On day 8, approximately 24 hours post-treatment, animals were sacrificed via CO_2
213 inhalation. The hindlimb was initially cleaned with chlorhexidine, and sterile instruments were
214 used to disarticulate the femur and adjacent soft tissues for further evaluation. For bacterial
215 counting, bone samples were initially minced using sterile bone rongeurs and further processed
216 using a homogenizer (Cole-Parmer, LabGEN7, 30s at setting 2-3, 30s at setting 9-10). Soft tissue
217 samples were minced using sterile surgical scissors, then homogenized (30s at setting 2-3, 30s at
218 setting 7-8). Following initial processing, homogenates were vortexed (2000 RPM, 1 minute),
219 diluted as necessary, spread onto BHI agar plates, and incubated for 24 hours at 37°C for
220 enumeration, with a detection limit set at 25-250 colonies.

221 **Fig 1. Overview of *in vivo* experimental procedure.** (A-B) On day 0 (infection surgery day), a
222 bicortical defect (drill hole) was generated in the mid-diaphysis of the left femur. A
223 contaminated orthopedic screw was then fastened into this space, and left for 7 days to generate
224 robust osteomyelitis and soft tissue infection. At day 7, the orthopedic screw was removed and
225 100µL of therapeutic(s) were injected into the defect space. At day 8, 24h after treatment, soft
226 tissues and bone samples were collected for histology, scanning electron microscopy, and
227 bacterial counts. (C) At days 1, 3, and 6, IVIS imaging was performed to track infection
228 progression.

229 Electron microscopy and histological analyses

230 Screw samples for electron microscopy analysis were collected during revision surgeries
231 on day 7 immediately prior to application of treatment, and placed directly into a fixative

232 consisting of 5% glutaraldehyde, 2% paraformaldehyde (w/w) in a sodium cacodylate buffer (a
233 modified "Karnovsky's" solution).[24] For electron microscopy analysis of infected bone, a
234 representative control femur (empty alginate group) was collected at day 8, broken along the
235 screw line with sterile bone rongeurs, and immediately placed in fixative for 24h. For both the
236 screw and bone samples, no dehydration series was performed in order to preserve the biofilm.
237 Prior to imaging, both samples were placed onto stubs with carbon tape and sputter coated
238 (Quorom Tech Model # SC7640) with platinum at 30 mA and 3.5 kV for 3-5 minutes. All
239 samples were then imaged using FESEM (Carl Zeiss AG-SUPRA 40).

240 For histological analyses, the infected femur and adjacent soft tissues were placed into
241 10% formalin for 48h, at ~20°C. Bone samples were decalcified for 5 days in Kristensen's
242 solution, then rinsed and placed into 10% formalin.[25] Tissues were routinely processed,
243 embedded in paraffin, sectioned at 5µm, and Gram or hematoxylin and eosin (H&E) stained.

244 Statistical analyses

245 All statistical analyses were performed using either GraphPad Prism 8 or SAS software
246 systems. For the Kirby-Bauer assay, a one-way analysis of variance (ANOVA) with Tukey's
247 multiple comparisons test was performed. For the *in vitro* antibiofilm assay, a two-way ANOVA
248 with Tukey's multiple comparisons were performed. For bacterial counts from directly prepared
249 and *ex vivo* orthopedic screws, a one-way ANOVA was performed, with Sidak's multiple
250 comparisons. All aforementioned statistical analyses were performed using GraphPad Prism 8
251 (GraphPad Software, Inc.). For bone and soft tissue *ex vivo* bacterial counts, general linear
252 models using PROC MIXED in SAS (SAS Institute, Inc.) were performed, with pairwise
253 comparisons using Tukey's (comparing treatment groups to one another) or Dunnett's

254 (comparing each treatment to control) tests. An alpha level of 0.05 was used to determine
255 statistical significance for all methods. Data are presented as mean ± standard deviation (SD).

256 Results

257 Integration of GFP into *S. aureus*

258 Longitudinal analyses of infection progression and regression is an ideal tool for new
259 model generation. Plasmids harboring reporter genes such as luminescence and fluorescence
260 have been most commonly used; however, it is necessary to constantly provide antibiotic
261 selective pressure to prevent a loss of plasmid, which is not achievable with *in vivo* models. In
262 this study, we integrated the GFP reporter gene into the genome of *S. aureus* ATCC 6538 strain
263 for the stable and accurate assessment of bacterial growth. All *S. aureus* ATCC 6538-GFP
264 colonies grown in BHI plates without antibiotic selective pressure were highly fluorogenic over a
265 span of 7 days (Fig. 2A). Furthermore, ATCC 6538-GFP recovered from an *ex vivo* orthopedic
266 screw at day 7 post-infection was still highly fluorogenic (Fig. 2B). These results demonstrated
267 that *S. aureus* ATCC 6538 chromosomally integrated with GFP can be used for real-time
268 monitoring of bacterial proliferation *in vitro* and *in vivo*.

269 **Fig 2. Integration of GFP into ATCC 6538.** (A) Phenotypic expression confirming integration
270 of GFP into ATCC 6538 was stable over a 7 day period. (B) A *Staphylococcus aureus* CFU
271 isolated from a contaminated screw *ex vivo* at day 7 revealed GFP expression continued after
272 growth over a week *in vivo*.

273 Kirby-Bauer analyses

274 For initial investigation of selected therapeutics, a Kirby-Bauer assay was performed
275 (Fig. 3A). All therapeutics—fosfomycin, phage, and dual—had a larger zone of inhibition than

276 the PBS control (“a”, $p<0.0001$), which generated no zone of inhibition (“N.D.”) Dual and
277 fosfomycin also resulted in a zone of inhibition greater than phage treatment (“b,” $p<0.0001$).
278 **Fig 3. *in vitro* Analyses of Therapeutic Bactericidal Activity.** (A) From the Kirby-Bauer assay,
279 all therapeutics delivered via PBS had a greater antibacterial effect than the PBS control (“a”,
280 $p<0.0001$), which generated no zone of inhibition (“N.D.”). Dual and fosfomycin therapeutics
281 also generated a zone of inhibition greater than phage treatment (“b,” $p<0.0001$). (B)
282 Vancomycin (256-1024 µg/mL), fosfomycin, (16-128 µg/mL) and bacteriophage (MOI 5-25)
283 delivered via PBS revealed varied bactericidal activity, where green indicated bacterial vitality
284 and black indicated a lack of bacterial presence. Interestingly, vancomycin appeared to have little
285 to no efficacy on biofilms at all concentrations. Fosfomycin, in contrast, showed efficacy at 64
286 and 128 µg/mL, a dose range approximately one-tenth the vancomycin doses utilized.
287 Bacteriophage was effective at an MOI of 10, indicated by the black panel revealing no viable *S.*
288 *aureus*. (C) Compared to the empty alginate group, alginate-loaded fosfomycin, phage, and dual
289 therapeutic-treated biofilms had lower bacterial loads at 6, 12, and 24 hours, except the
290 fosfomycin group at 6 hours (“c,” $p<0.05$). Interestingly, all groups (fosfomycin, phage, dual,
291 and empty alginate gel) had lower growth at all time points compared to the PBS control, i.e. the
292 empty alginate gel exerted a killing effect (“s,” $p<0.05$). Within individual treatment groups over
293 time, increased antimicrobial effects were observed. The fosfomycin treated biofilms were
294 different at 6 and 12 hours, and at 12 and 24 hours (**$p<0.0001$). Phage treated groups were
295 different at 6 and 12 hours, and at 6 and 24 hours (*$p<0.05$). Dual treated biofilms were different
296 at 6 and 12 hours, at 6 and 24 hours, and at 12 and 24h (**$p<0.0001$). The empty alginate and
297 PBS controls resulted in no changes over time.
298

299 **Qualitative and quantitative bactericidal activity on biofilms**

300 Biofilms are generally considered the greatest agent of osteomyelitis treatment failure,
301 and thus are important to consider when developing therapeutics. For this reason, it is important
302 to evaluate the efficacy of novel therapeutics on robust biofilms, for translation into relevant
303 clinical scenarios. Antibiofilm efficacy of therapeutics *in vitro* was characterized utilizing two
304 different analyses: (i) qualitative fluorescent (phenotypic) assessment and (ii) quantitative
305 bacterial counting. Surprisingly, vancomycin, one of the most commonly utilized antibiotics for
306 difficult osteomyelitis cases, appeared to have little or no effect on biofilms, as indicated by the
307 presence of green fluorescing *S. aureus* (Fig. 3B). Fosfomycin is a small molecular weight (138
308 g/mol) broad-spectrum antibiotic and promising therapeutic option against biofilm.[26] Here,
309 fosfomycin appeared to remove biofilm at 64 and 128 μg/mL, doses much lower than
310 vancomycin. The CRISPR-Cas9 modified bacteriophage has dual killing mechanisms: (i) a direct
311 lysis of target bacteria by holin or murein hydrolase, and (ii) CRISPR-Cas9 nuclease activity.
312 From qualitative fluorescent analyses, it was determined than a phage MOI of ~10 was effective
313 in clearing biofilm infection (Fig. 3B).

314 Alginate is a versatile biopolymer used for prolonged, localized availability of
315 therapeutic.[27] Antibiofilm assays with bacterial counts were utilized to qualitatively assess the
316 effects over time of selected therapeutics delivered via alginate (Fig. 3C). Compared to the
317 empty alginate group, fosfomycin, phage, and dual therapeutic-treated biofilms had significantly
318 lower bacterial loads at 6, 12, and 24 hours, except the fosfomycin group at 6 hours ("c,"
319 $p<0.05$). Interestingly, all groups (fosfomycin, phage, dual, and empty alginate gel) were
320 significantly lower at all time points compared to the PBS treatment, i.e. the empty alginate gel
321 exerted a killing effect ("s", $p<0.05$). In all treatment groups where alginate was loaded with

322 therapeutic(s), antibiofilm effects increased over time. The fosfomycin treated biofilms were
323 different at 6 and 12 hours, and at 12 and 24 hours (**$p<0.0001$). Phage treated groups were
324 different at 6 and 12 hours, and at 6 and 24 hours (*$p<0.05$). Dual treated biofilms were different
325 at 6 and 12 hours, at 6 and 24 hours, and at 12 and 24h (**$p<0.0001$). As expected, the empty
326 alginate and PBS controls did not change over time.

327 Bacterial load on orthopedic screws

328 To generate consistent infection in the osteomyelitis model, contaminated orthopedic
329 screw preparation had to first be characterized. Two parameters of screw preparation were
330 evaluated: soak time and dry time. Soak time (5-20 min) of screws appeared to increase
331 somewhat proportionally with respect to bacterial load (Fig. 4A). Dry times from 0-10 min
332 appeared to have little effect on bacterial load; at 20 min, decreased viability of *S. aureus* was
333 observed (Fig. 4B).

334 In the *in vivo* model, orthopedic screws removed at day 7 to allow injection of therapeutic
335 into the infected defect space were analyzed for bacterial load to confirm all treatment groups
336 began with a similar extent of infection. Bacterial counts from *ex vivo* screws indicated similarly
337 severe infection among all samples (treated immediately following), with an average 8.19×10^4
338 CFU/mL bacterial load (Fig. 4C). Per what would become individual treatment groups,
339 calculated averages were: 1.05×10^5, 7.50×10^4, 8.20×10^4, and 6.57×10^4 for fosfomycin, phage,
340 dual, and control groups, respectively. No significant differences between any groups were
341 observed.

342 **Fig 4. Effect of soak time and dry time on bacterial load of orthopedic screws**. (A) Soak time
343 of sterile orthopedic screws in *Staphylococcus aureus* appeared to linearly relate to ultimate
344 bacterial load. (B) Dry time did not appear to decrease ultimate bacterial load, until 20 minutes

345 of dry time. (A-B) The ranges of soak time and dry time used for preparation of screws for the *in*
346 *vivo* study are indicated by the red portions of the x-axes. The average time for soak and dry
347 times for orthopedic screws used *in vivo* is marked by an "x". (C) Bacterial counts collected
348 from orthopedic screws at day 7 *ex vivo* indicated a similar ultimate bacterial load among what
349 would become different treatment groups.

350 **Scanning Electron Microscopy**

351 Representative SEM images of screws collected at day 7 post-infection revealed an
352 abundance of gram positive cocci (*S. aureus*), as expected, along the distal portion of the screw
353 and within the ridges of the screw throughout its length (Fig. 5A-B). In bone fragments collected
354 along the screw line (defect site) of an untreated (empty alginate) control sample at day 8 (24h
355 post-treatment), gram positive cocci, presumably *S. aureus,* were visible. (Fig. 5C-D).

356 **Fig 5. Bacteria on *ex vivo* orthopedic screws and bone**. (A-B) Gram positive cocci, and what
357 appears to be biofilm, was evident on the distal portion (A) and between threads (B) of an *ex vivo*
358 orthopedic screw excised at day 7. (C-D). Femur sample adjacent to the defect/screw site
359 collected at day 8 from untreated (empty alginate) control revealed dispersed gram positive
360 cocci.

361 **Bacterial load within bone and soft tissue**

362 The average bone bacterial counts per treatment group were as follows: (i) control: 4.197
363 ± 0.289, (ii) fosfomycin: 3.401 ± 0.924, (iii) phage: 4.076 ± 0.268, and (iv) dual: 3.607 ± 0.316
364 (Log_{10}(CFU)), Fig. 6A). Fosfomycin bacterial counts were lower than empty alginate control
365 (p=0.0083) and phage (p=0.0486).

366 The average soft tissue bacterial counts per treatment group were as follows: (i) control:
367 4.713 ± 0.331, (ii) fosfomycin: 4.146 ± 0.377, (iii) phage: 4.160 ± 0.516, and (iv) dual: 4.201 ±

368 0.556 (Log_{10}(CFU)), Fig. 6B). Bacterial counts were lower in fosfomycin (p=0.0225), phage
369 (0.0265), and dual (p=0.0430) treated groups compared to empty alginate control.
370 **Fig 6. Bacterial counts from bone and soft tissue.** (A) Bacterial counts from bone tissue
371 harvested from fosfomycin treated animals were lower than those for empty alginate
372 (**p=0.0083) and phage (*p=0.0486) groups. (B) In soft tissue, bacterial loads were reduced in
373 all three treatment groups—fosfomycin (*p=0.0225), phage (*p=0.0265), and dual
374 (*p=0.0430)—compared to empty alginate.

375 ## Histology

376 Bone samples stained with H&E or Gram revealed strong evidence for development of a
377 severe osteomyelitis infection. The areas at the site of the screw were characterized by extensive
378 remodeling within the medullary cavity, with replacement of marrow cells by a central area of
379 neutrophils surrounded by fibrovascular proliferation and reactive bone. Within the cortex, at the
380 site of screw placement, was mild bone necrosis characterized by empty lacunae and bone loss.
381 Along the periosteal surface there was locally extensive proliferation of woven bone (periosteal
382 proliferation). Additionally, abundant gram-positive cocci were localized within the bone. No
383 differences in the extent of infection among any groups were apparent. The outcome of the
384 fosfomycin-treated bone histology varied from the other samples, due to sample damage during
385 processing. Ultimately, this prevented the collection of images along the screw line (where the
386 majority of bacteria and inflammation were localized), as seen with the other groups. However,
387 the proliferation of woven bone, as a reactive process on the cortical surface, is visible (Fig. 7B).
388 Within the phage-treated bone sample, a linear track of gram-positive bacteria in the bone at the
389 original site of the screw line was visible (Fig. 7C). In the dual-treated sample, neutrophilic
390 inflammation surrounded by reactive bone and fibrosis was observed (Fig.7D left, *).

391

392 **Fig 7. Histology of infected bones one day post-treatment**. (A, left) At the site of the screw of
393 the empty alginate control was marked neutrophilic inflammation (arrows) with bone loss,
394 surrounded by reactive bone and fibrosis (*, bar=50µm). (A, right) A higher magnification of the
395 area of bone loss with large numbers of neutrophils (bar=5µm). Inset demonstrating gram
396 positive bacteria within and outside macrophages (arrow, bar=5µm). (B) Within the fosfomycin
397 treated bone, periosteal proliferation of woven bone was noted (arrows, bar=50µm). (C, left) A
398 linear track in the bone at the site of the screw (arrows) with abundant neutrophils and reactive
399 bone and fibrosis was observed (arrows, H&E, bar=5µm). (C, right) Gram staining
400 demonstrating aggregates of basophilic bacteria along the screw site (bar=50µm). Inset is a
401 higher magnification of the bacteria (bar=5µm). (D, left) At the site of the screw was marked
402 neutrophilic inflammation with bone loss (arrows), surrounded by reactive bone and fibrosis (*,
403 bar=50µm). (D, right) A higher magnification of the area of bone loss with large numbers of
404 neutrophils (bar=50µm). Inset demonstrating gram positive bacteria within and outside
405 macrophages (arrow, bar=5µm).

406 # Discussion

407 In this manuscript, a previously developed CRISPR-Cas9 modified bacteriophage
408 therapeutic, which was successful in treating external dermal infection[21], was evaluated as a
409 therapeutic for internal osteomyelitis and contiguous soft tissue infection in a rat model using a
410 biofilm forming strain of *S. aureus*. For real time monitoring of *S. aureus,* GFP was
411 chromosomally integrated into *S. aureus* ATCC 6538 strain by homologous recombination. We
412 demonstrated that *S. aureus* ATCC 6538 strain carrying the GFP gene stably maintained the GFP
413 phenotype without antibiotic selective pressure *in vitro* and *in vivo*.

414 The therapeutic effects of vancomycin, fosfomycin, CRISPR-Cas9 modified
415 bacteriophage, and fosfomycin-bacteriophage dual treatments were evaluated against biofilm *in*
416 *vitro*. Vancomycin is considered a last resort treatment for *S. aureus* infection. Recent guidelines
417 recommend vancomycin trough concentrations between 15 and 20 µg/mL for effectively
418 controlling *S. aureus* infection.[28] As biofilms are typically more difficult to treat than
419 planktonic bacteria, a much higher concentration of vancomycin (256-1024 µg/mL) was used
420 here. Although the planktonic *S. aureus* ATCC 6538 strain was sensitive to vancomycin at 2
421 µg/mL within BHI broth (data not shown), in biofilm form, it was highly resistant to vancomycin
422 even at 1024 µg/mL. Biofilms consist of a group of bacteria and their byproducts such as
423 extracellular polymeric substances (EPS) including proteins, DNA, RNA, polysaccharides, and
424 peptidoglycans. These EPS materials provide physical barriers to penetration of antibiotics to the
425 inner viable population of bacteria in the biofilm. Vancomycin, a large glycopeptide antibiotic
426 with a molecular weight of 1,449 g/mol, binds to the D-ala-D-ala terminal amino acid at the stem
427 of pentapeptide crosslinking peptidoglycan for efficacy[29]. Thus, resistance to vancomycin by
428 biofilm may be explained by poor penetration of vancomycin due to its bulky size, which could
429 have led to entrapment at the peptidoglycan layer of biofilm. In contrast, fosfomycin showed
430 better efficacy against biofilm at much lower (64 and 128 µg/mL) doses. Fosfomycin is a small
431 bactericidal antibiotic with a molecular weight of 138 g/mol. It interferes with the first step of
432 peptidoglycan synthesis by inhibiting the phosphoenolpyruvate synthetase[30]. Thus, the
433 enhanced fosfomycin efficacy could be explained by better penetration of fosfomycin due to its
434 small size and its inhibition of the first step of peptidoglycan synthesis. From qualitative
435 fluorescent analyses, it was determined than a phage MOI of ~10 was effective in clearing
436 biofilm infection. This is similar and in some cases an improvement upon *in vitro* evaluation of

437 phage treatments discussed in literature, with biofilm eradication reported with MOI 10-
438 100.[21,31,32] Alginate hydrogel served as an effective delivery vehicle, enabling increasing
439 effects against biofilm over a 24h period, for fosfomycin, phage, and dual treatments *in vitro*.
440 Previously, we have observed similar sustained effects of bone morphogenetic protein-2 released
441 from and retained within alginate hydrogels *in vitro* and *in vivo*.[18,27]

442 For further evaluation of the CRISPR-Cas9 phage, motivated by augmented *in vitro*
443 efficacy relative to antibiotic controls, we developed a clinically relevant model of implant-
444 related osteomyelitis. In human cases of osteomyelitis, chronic infection is diagnosed after a 6-
445 week period of infection, while our model had only a 1-week infection period. Based on SEM
446 images, 1 week appeared to be sufficient to induce severe infection, including biofilm, in this rat
447 model. By culturing *S. aureus* on orthopedic screws, infection was localized to the femur and
448 surrounding soft tissue, as indicated by fluorescent imaging and histology. Fluorescent imaging
449 served as a qualitative tool for longitudinal infection progression/regression, although no direct
450 correlation between radiance output and bacterial load were observed (data not shown). This
451 could be attributed at least in part to a residual GFP signal that likely exists after bacterial cell
452 death, due to the persistence of the GFP. Clinically, debridement accompanied by long-term
453 antibiotic administration is the gold standard for osteomyelitis treatment.[33] In this study, we
454 have avoided debridement altogether so as to limit potential clearing of infection from any
455 source other than the therapeutics delivered. For future studies, debridement may be included to
456 more readily mimic the clinical scenario and enable evaluation of larger antibacterial materials
457 such as scaffolds or putties.

458 From bacterial counts performed on excised soft tissues, it was determined that severe
459 soft tissue infection accompanied the expected high bacterial load in the bone samples. In

460 clinical cases of osteomyelitis, soft tissue infection is a common pathological finding of
461 osteomyelitis infection progression[34–36]. In this model, soft tissue infection likely developed
462 due to the distal end of the orthopedic screw resting freely within the soft tissue medial to the
463 defect site. On excised orthopedic screws collected on day 7, scanning electron microscopy
464 indicated a purulent, thick biofilm layer of *Staphylococci* on the end of the orthopedic screw.
465 Based on *in vitro* results, the process of orthopedic screw preparation can be used to tailor the
466 extent of infection, as soaking the screws for a shorter period of time would be expected to
467 introduce less *S. aureus* into the bone and as a result induce a less severe infection. Histology
468 results support the development of severe osteomyelitis infection, with disease hallmarks such as
469 neutrophilic inflammation, reactive bone, fibrosis, and gram-positive bacteria. Within the 24-
470 hour time frame of this study, no differences among treatment groups were apparent. If later time
471 points were evaluated, the differences noted in bacterial counting would likely be more readily
472 reflected histologically.

473 Although only the fosfomycin group resulted in reduced bacterial load in the femur, in
474 soft tissue, all three treatments, including phage alone and phage with fosfomycin (dual) led to
475 lower bacterial counts compared to empty alginate. It should be noted than an extremely high
476 dose of fosfomycin (3g) was administered to the rat femur in this study. In humans, a 3g oral
477 dose is recommended for treatment of urinary tract infections.[26] Conversely for bacteriophage
478 dose, although a minimum effective MOI of ~10 was observed *in vitro*, *in vivo* only MOI of ~3
479 was able to be delivered due to: (i) the volume of alginate hydrogel delivered to the small defect
480 site (100 μL total, but only ~10 μL fit into the defect itself), and (ii) the thicker consistency of
481 phage solution, limiting the concentration that could be prepared in alginate hydrogel.
482 Collectively, these discrepancies in dosing likely limited the efficacy of phage treatment alone in

483 osteomyelitis mitigation relative to antibiotic with and without phage. Furthermore, the
484 canaliculi of cortical bone may provide an ideal environment for bacteria to evade treatment.[37]
485 It should also be noted that in this study, a one-time 100 μL treatment was applied locally.
486 Clinically, osteomyelitis is treated via debridement and systemic antibiotics for several
487 weeks.[33] Similarly, success with bacteriophage therapy has been associated with continuous,
488 prolonged delivery of the virus. A bacteriophage cocktail was used to successfully clear femoral
489 infection with four intraperitoneal doses of phage (100 μL of ~$2x10^{12}$ plaque forming units
490 (PFU)/mL) over the span of 48 hours.[38] Another study adopted a treatment regimen for tibial
491 osteomyelitis consisting of a once daily $3x10^{8}$ PFU/mL intramuscular bacteriophage injection for
492 14 days, which resolved the infection.[39] Recently, a case report was published describing the
493 success of a weekly injection of bacteriophage over a seven-week period for human digital
494 osteomyelitis.[36] Collectively, these data suggest that sustained, localized concentrations of
495 phage may be necessary for efficacy in treatment of bone infection. In future studies, a greater
496 initial dose of phage therapeutic should be considered, or a longer duration of treatment achieved
497 with a delivery vehicle capable of tailored release of therapeutic. Given a higher phage dose
498 and/or prolonged availability, it is possible that the efficacy of phage observed here *in vitro* could
499 be matched *in vivo*. Furthermore, it may be more advantageous to use alternating doses of the
500 antibiotic and phage therapeutic over time, rather than a combined simultaneous
501 application.[40,41] In this study, no additive effect of fosfomycin or phage was observed in the
502 dual treatment group. Only a 24h treatment period was evaluated, which may have limited the
503 effect of our selected therapeutics, as later time points may have allowed therapeutics, especially
504 those containing phages (which must replicate for optimal bactericidal activity), to have a

505 cumulative effect. Nonetheless, our challenging composite tissue infection model enabled
506 efficient, rapid testing of antimicrobial therapeutics using a biofilm forming strain of *S. aureus*.
507 Despite the prevalence and severity of osteomyelitis, no bacteriophage-based treatment
508 for the disease has reached clinical trials in the United States. As populations of MDR-bacteria
509 continue to spread and new strains are isolated, engineering novel therapeutics will be essential
510 to augment the dwindling list of effective, available antibiotics. Phage therapy has great potential
511 to fill this niche, as phages can be made readily and at a low cost. Using CRISPR-Cas9
512 technology as in this study, phages can be modified to have a wide host range.[21] By
513 contributing to the pipeline of bacteriophage therapeutic evaluation compared to traditional
514 antibiotics, the goal of this work was to demonstrate efficacy of phage against bone and soft
515 tissue infection. Enhanced bactericidal activity of CRISPR-Cas9 phage was demonstrated *in*
516 *vitro* against biofilm, when compared to conventionally used vancomycin and fosfomycin
517 antibiotics. Subsequently, an implant-related model of osteomyelitis and soft tissue infection was
518 established, confirmed with histological, radiographic, and scanning electron microscopy
519 analyses. Although phage did not mitigate bone infection 24h post-treatment, soft tissue infection
520 was reduced 24h following treatment with bacteriophage, and notably to the same extent as
521 treatment with high dose antibiotic. To improve bacteriological outcomes in the future, further
522 investigations of delivery vehicles and optimal dosing are warranted.

523 **Acknowledgements**

524 This research was supported by the NIH Center of Biomedical Research Excellence in Pathogen-
525 Host Interactions (2P20GM103646) and the Office of Research and Economic Development at
526 Mississippi State University. The authors would like to thank Dr. Jean Feugang, Dr. Seongbin
527 Park, and the USDA-ARS Biophotonics Initiative (58-6402-3-018) for supporting our use of the

528 IVIS Lumina XR system, Dr. Robert Wills for statistical analyses, and Dr. Lucy Senter and Dr.
529 Bridget Willeford for veterinary care. Thanks also to Jamie Walker, Delisa Pennell, Dr. Hayley
530 Gallaher, Weitong Chen, Kali Sebastian, Kristen Lacy, Christine Grant, Drew Moran, Ryan
531 Yingling, Alex Feaster, Hannah Bostick, Christina Moffett, Sonja Jensen, Anna Marie Dulaney,
532 and Luke Tucker for assistance with surgeries.

533 # Citations

534 1. Center for Disease Control and Prevention. Antibiotic Use in the United States, 2017:
535 Progress and Opportunities. US Dep Heal Hum Serv . 2017;
536 doi:10.1073/pnas.1417106112
537 2. Thorpe KE, Joski P, Johnston KJ. Antibiotic-Resistant Infection Treatment Costs Have
538 Doubled Since 2002, Now Exceeding $2 Billion Annually. Health Aff (Millwood). United
539 States; 2018;37: 662–669. doi:10.1377/hlthaff.2017.1153
540 3. O'Neill J. Antimicrobial Resistance : Tackling a crisis for the health and wealth of nations.
541 Rev Antimicrob Resist. 2014;
542 4. Tom Frieden. Antibiotic Resistance Threats. Cdc. 2013; doi:CS239559-B
543 5. Archer NK, Mazaitis MJ, William Costerton J, Leid JG, Powers ME, Shirtliff ME.
544 Staphylococcus aureus biofilms: Properties, regulation and roles in human disease.
545 Virulence. 2011. doi:10.4161/viru.2.5.17724
546 6. Johnson CT, Wroe JA, Agarwal R, Martin KE, Guldberg RE, Donlan RM, et al. Hydrogel
547 delivery of lysostaphin eliminates orthopedic implant infection by *Staphylococcus aureus*
548 and supports fracture healing. Proc Natl Acad Sci. 2018; doi:10.1073/pnas.1801013115
549 7. Geraghty T, LaPorta G. Current health and economic burden of chronic diabetic
550 osteomyelitis. Expert Review of Pharmacoeconomics and Outcomes Research. 2019.

551 doi:10.1080/14737167.2019.1567337

552 8. Rowley WR, Bezold C, Arikan Y, Byrne E, Krohe S. Diabetes 2030: Insights from
553 Yesterday, Today, and Future Trends. Popul Health Manag. 2017;
554 doi:10.1089/pop.2015.0181

555 9. Abatángelo V, Peressutti Bacci N, Boncompain CA, Amadio AA, Carrasco S, Suárez CA,
556 et al. Broad-range lytic bacteriophages that kill Staphylococcus aureus local field strains.
557 PLoS One. 2017; doi:10.1371/journal.pone.0181671

558 10. Tang Z, Huang X, Sabour PM, Chambers JR, Wang Q. Preparation and characterization of
559 dry powder bacteriophage K for intestinal delivery through oral administration. LWT -
560 Food Sci Technol. 2015; doi:10.1016/j.lwt.2014.08.012

561 11. Furfaro LL, Payne MS, Chang BJ. Bacteriophage Therapy: Clinical Trials and Regulatory
562 Hurdles. Front Cell Infect Microbiol. 2018; doi:10.3389/fcimb.2018.00376

563 12. Wright A, Hawkins CH, Änggård EE, Harper DR. A controlled clinical trial of a
564 therapeutic bacteriophage preparation in chronic otitis due to antibiotic-resistant
565 Pseudomonas aeruginosa; a preliminary report of efficacy. Clin Otolaryngol.
566 Wiley/Blackwell (10.1111); 2009;34: 349–357. doi:10.1111/j.1749-4486.2009.01973.x

567 13. Leitner L, Sybesma W, Chanishvili N, Goderdzishvili M, Chkhotua A, Ujmajuridze A, et
568 al. Bacteriophages for treating urinary tract infections in patients undergoing transurethral
569 resection of the prostate: A randomized, placebo-controlled, double-blind clinical trial.
570 BMC Urol. 2017; doi:10.1186/s12894-017-0283-6

571 14. Fabijan AP, Lin RCY, Ho J, Maddocks S, Iredell JR. Safety and Tolerability of
572 Bacteriophage Therapy in Severe Staphylococcus aureus
573 Infection. bioRxiv. 2019; 619999. doi:10.1101/619999

574 15. Voelker R. FDA Approves Bacteriophage TrialFDA Approves Bacteriophage TrialNews
575 From the Food and Drug Administration. JAMA. 2019;321: 638.
576 doi:10.1001/jama.2019.0510
577 16. Johnson C, Dinjaski N, Prieto M, García A. Bacteriophage Encapsulation in
578 Poly(Ethylene Glycol) Hydrogels Significantly Reduces Bacteria Numbers in an Implant-
579 Associated Infection Model of Bone Repair. Igarss 2014. 2014; doi:10.1007/s13398-014-
580 0173-7.2
581 17. Bean JE, Alves DR, Laabei M, Esteban PP, Thet NT, Enright MC, et al. Triggered
582 Release of Bacteriophage K from Agarose/Hyaluronan Hydrogel Matrixes by
583 Staphylococcus aureus Virulence Factors [Internet]. CHEMISTRY OF MATERIALS. pp.
584 7201–7208. doi:10.1021/cm503974g
585 18. Priddy LB, Chaudhuri O, Stevens HY, Krishnan L, Uhrig BA, Willett NJ, et al. Oxidized
586 alginate hydrogels for bone morphogenetic protein-2 delivery in long bone defects. Acta
587 Biomater. 2014/06/17. 2014;10: 4390–4399. doi:10.1016/j.actbio.2014.06.015
588 19. Krishnan L, Priddy LB, Esancy C, Li MTA, Stevens HY, Jiang X, et al. Hydrogel-based
589 Delivery of rhBMP-2 Improves Healing of Large Bone Defects Compared With
590 Autograft. Clin Orthop Relat Res. 2015; doi:10.1007/s11999-015-4312-z
591 20. Souza GR, Yonel-Gumruk E, Fan D, Easley J, Rangel R, Guzman-Rojas L, et al. Bottom-
592 up assembly of hydrogels from bacteriophage and Au nanoparticles: The effect of Cis-
593 and trans-acting factors. PLoS One. 2008; doi:10.1371/journal.pone.0002242
594 21. Park JY, Moon BY, Park JW, Thornton JA, Park YH, Seo KS. Genetic engineering of a
595 temperate phage-based delivery system for CRISPR/Cas9 antimicrobials against
596 Staphylococcus aureus. Sci Rep. The Author(s); 2017;7: 44929. Available:

597 http://dx.doi.org/10.1038/srep44929
598 22. De Jong NWM, Van Der Horst T, Van Strijp JAG, Nijland R. Fluorescent reporters for
599 markerless genomic integration in Staphylococcus aureus. Sci Rep. 2017;
600 doi:10.1038/srep43889
601 23. Bauer AW, Kirby WM, Sherris JC, Turck M. Antibiotic susceptibility testing by a
602 standardized single disk method. Am J Clin Pathol. England; 1966;45: 493–496.
603 24. Karnovsky MJ. A Formaldehyde-Glutaraldehyde Fixative of High Osmolality for Use in
604 Electron Microscopy. The American Society for Cell Biology Source: The Journal of Cell
605 Biology. 1965.
606 25. Kristensen HK. An Improved Method of Decalcification. Stain Technol. Taylor &
607 Francis; 1948;23: 151–154. doi:10.3109/10520294809106242
608 26. Dijkmans AC, Zacarías NVO, Burggraaf J, Mouton JW, Wilms E, van Nieuwkoop C, et
609 al. Fosfomycin: Pharmacological, Clinical and Future Perspectives. Antibiotics. 2017;
610 doi:10.3390/antibiotics6040024
611 27. Krishnan L, Priddy LB, Esancy C, Klosterhoff BS, Stevens HY, Tran L, et al. Delivery
612 vehicle effects on bone regeneration and heterotopic ossification induced by high dose
613 BMP-2. Acta Biomater. 2017; doi:10.1016/j.actbio.2016.12.012
614 28. Lodise TP, Lomaestro B, Graves J, Drusano GL. Larger vancomycin doses (at least four
615 grams per day) are associated with an increased incidence of nephrotoxicity. Antimicrob
616 Agents Chemother. 2008; doi:10.1128/AAC.01602-07
617 29. Wang F, Zhou H, Olademehin OP, Kim SJ, Tao P. Insights into key interactions between
618 vancomycin and bacterial cell wall structures. ACS Omega. 2018;
619 doi:10.1021/acsomega.7b01483

620 30. Takahata S, Ida T, Hiraishi T, Sakakibara S, Maebashi K, Terada S, et al. Molecular
621 mechanisms of fosfomycin resistance in clinical isolates of Escherichia coli. Int J
622 Antimicrob Agents. 2010; doi:10.1016/j.ijantimicag.2009.11.011
623 31. Alves DR, Gaudion A, Bean JE, Perez Esteban P, Arnot TC, Harper DR, et al. Combined
624 Use of Bacteriophage K and a Novel Bacteriophage To Reduce Staphylococcus aureus
625 Biofilm Formation. Appl Environ Microbiol. 2014; doi:10.1128/aem.01789-14
626 32. Pincus NB, Reckhow JD, Saleem D, Jammeh ML, Datta SK, Myles IA. Strain specific
627 phage treatment for Staphylococcus aureus infection is influenced by host immunity and
628 site of infection. PLoS One. 2015; doi:10.1371/journal.pone.0124280
629 33. Nelson CL, McLaren SG, Skinner RA, Smeltzer MS, Thomas JR, Olsen KM. The
630 treatment of experimental osteomyelitis by surgical debridement and the implantation of
631 calcium sulfate tobramycin pellets. J Orthop Res. 2002; doi:10.1016/S0736-
632 0266(01)00133-4
633 34. Taki H, Krkovic M, Moore E, Abood A, Norrish A. Chronic long bone osteomyelitis:
634 diagnosis, management and current trends. Br J Hosp Med. 2016;
635 doi:10.12968/hmed.2016.77.10.c161
636 35. Berbari EF, Kanj SS, Kowalski TJ, Darouiche RO, Widmer AF, Schmitt SK, et al. 2015
637 Infectious Diseases Society of America (IDSA) Clinical Practice Guidelines for the
638 Diagnosis and Treatment of Native Vertebral Osteomyelitis in Adults[a]. Clinical Infectious
639 Diseases. 2015. doi:10.1093/cid/civ633
640 36. Fish R, Kutter E, Bryan D, Wheat G, Kuhl S. Resolving Digital Staphylococcal
641 Osteomyelitis Using Bacteriophage—A Case Report. Antibiotics. 2018;
642 doi:10.3390/antibiotics7040087

643 37. de Mesy Bentley KL, Trombetta R, Nishitani K, Bello-Irizarry SN, Ninomiya M, Zhang
644 L, et al. Evidence of Staphylococcus Aureus Deformation, Proliferation, and Migration in
645 Canaliculi of Live Cortical Bone in Murine Models of Osteomyelitis. J Bone Miner Res.
646 2017; doi:10.1002/jbmr.3055
647 38. Kishor C, Mishra RR, Saraf SK, Kumar M, Srivastav AK, Nath G. Phage therapy of
648 staphylococcal chronic osteomyelitis in experimental animal model. Indian J Med Res.
649 2016; doi:10.4103/0971-5916.178615
650 39. Ibrahim OMS, Sarhan SR, Salih SI. Activity of Isolated Staphylococcal Bacteriophage in
651 Treatment of Experimentally Induced Chronic Osteomyelitis in Rabbits. Adv Anim Vet
652 Sci. 2016; doi:10.14737/journal.aavs/2016/4.11.593.603
653 40. Lopes A, Pereira C, Almeida A. Sequential Combined Effect of Phages and Antibiotics on
654 the Inactivation of Escherichia coli. Microorganisms. MDPI; 2018;6: 125.
655 doi:10.3390/microorganisms6040125
656 41. Tagliaferri TL, Jansen M, Horz H-P. Fighting Pathogenic Bacteria on Two Fronts: Phages
657 and Antibiotics as Combined Strategy [Internet]. Frontiers in Cellular and Infection
658 Microbiology . 2019. p. 22. Available:
659 https://www.frontiersin.org/article/10.3389/fcimb.2019.00022
660

Figure 1

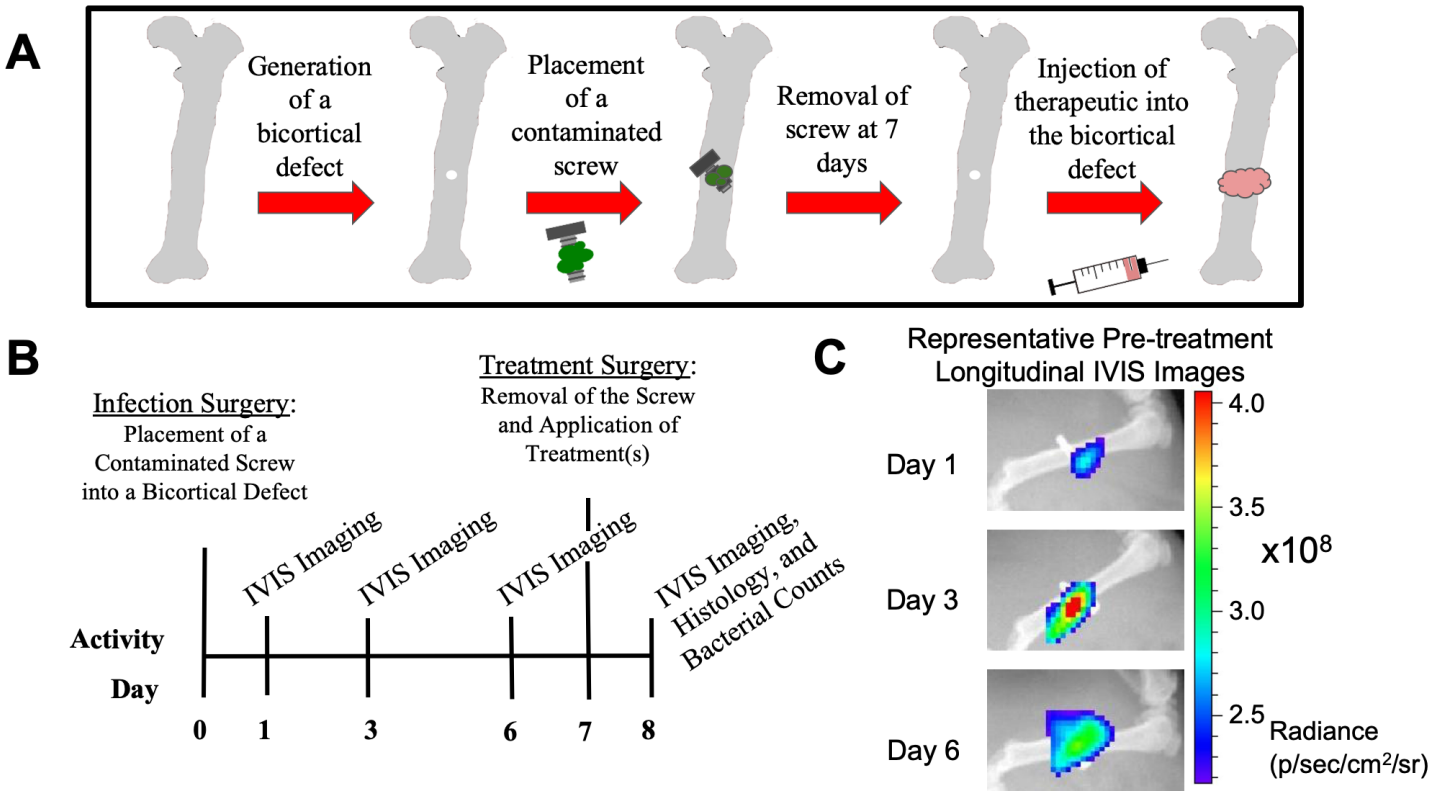
A
Generation of a bicortical defect
Placement of a contaminated screw
Removal of screw at 7 days
Injection of therapeutic into the bicortical defect
B
Infection Surgery: Placement of a Contaminated Screw into a Bicortical Defect
Treatment Surgery: Removal of the Screw and Application of Treatment(s)
IVIS Imaging
IVIS Imaging
IVIS Imaging
IVIS Imaging, Histology, and Bacterial Counts
Activity
Day
0
1
3
6
7
8
C
Representative Pre-treatment Longitudinal IVIS Images
Day 1
Day 3
Day 6
4.0
3.5
3.0
2.5
x10^8
Radiance (p/sec/cm^2/sr)

Figure 2

A ***in vitro* stability of ATCC 6538-GFP**

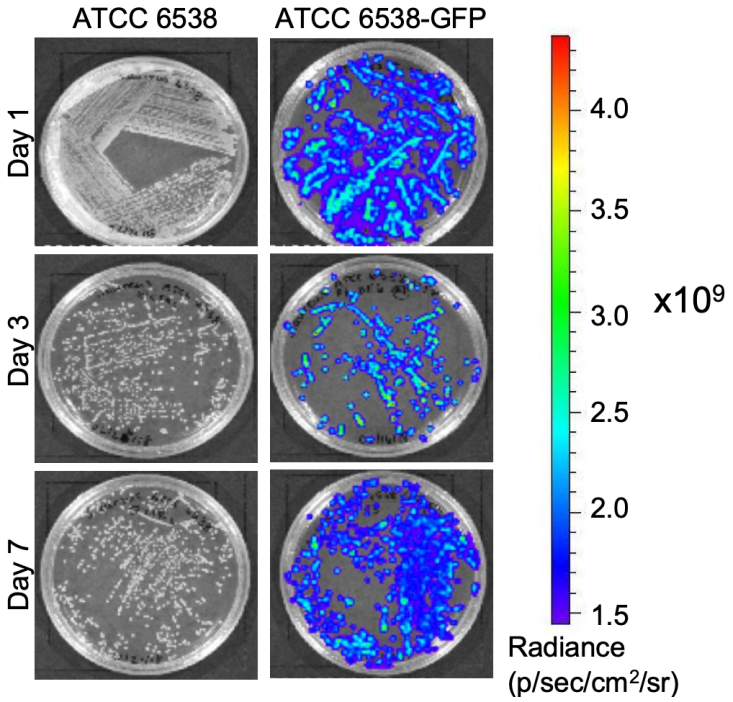

B ***ex vivo stability* of ATCC 6538-GFP**

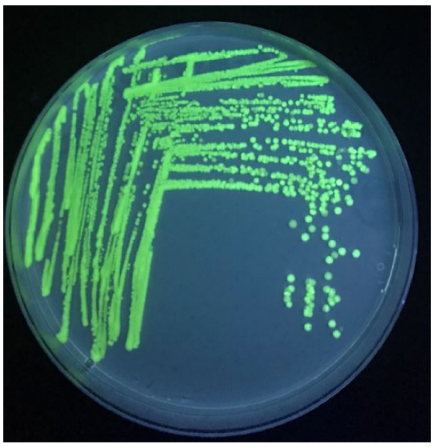

Figure 3

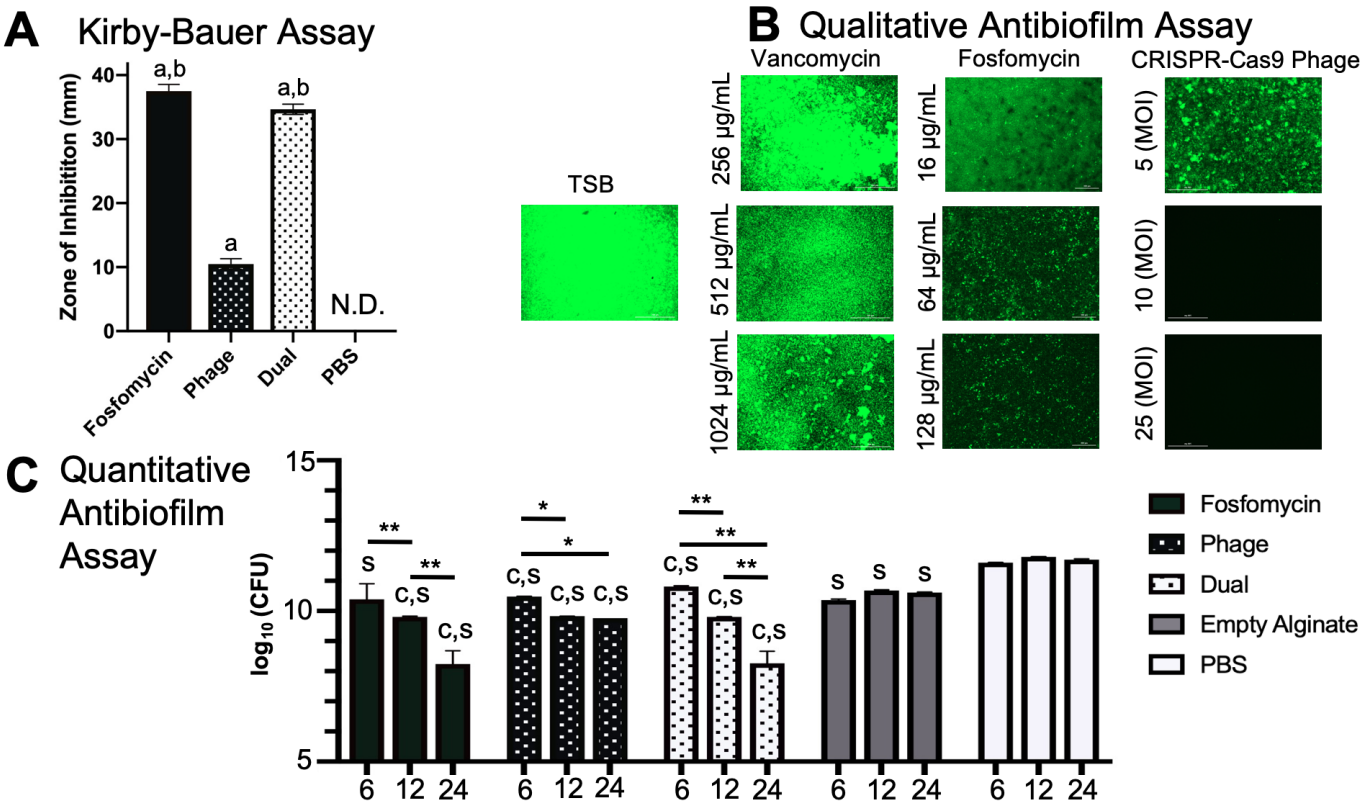
A Kirby-Bauer Assay
Zone of Inhibititon (mm)
40
30
20
10
0
a,b
a
a,b
N.D.
Fosfomycin
Phage
Dual
PBS
TSB
B Qualitative Antibiofilm Assay
Vancomycin
Fosfomycin
CRISPR-Cas9 Phage
256 µg/mL
512 µg/mL
1024 µg/mL
16 µg/mL
64 µg/mL
128 µg/mL
5 (MOI)
10 (MOI)
25 (MOI)
C Quantitative Antibiofilm Assay
log10 (CFU)
15
10
5
6 12 24
Fosfomycin
Phage
Dual
Empty Alginate
PBS

Figure 4

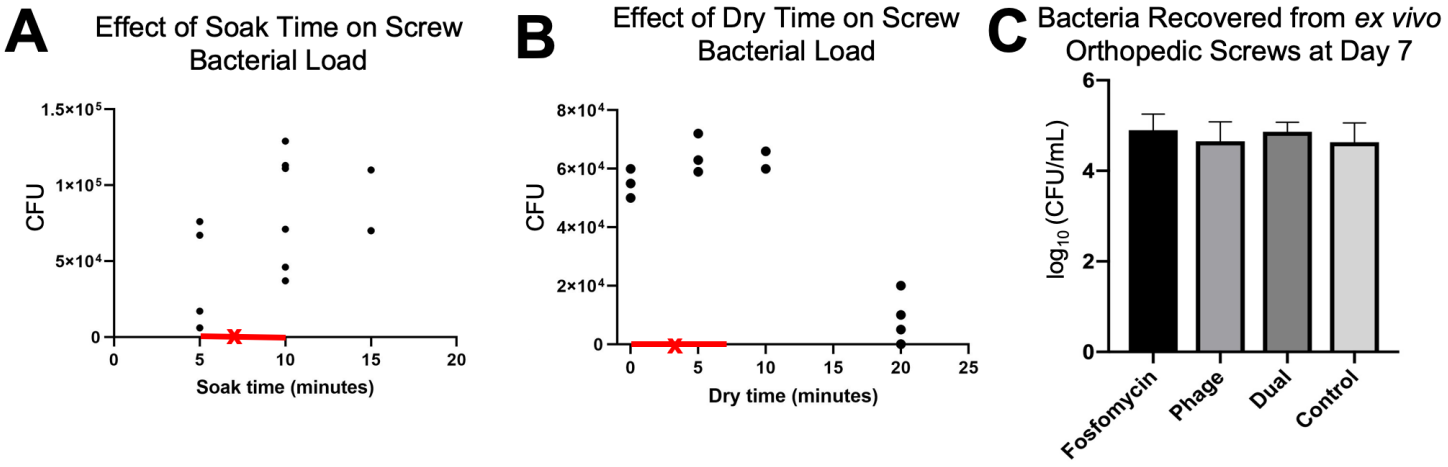
A
Effect of Soak Time on Screw Bacterial Load
CFU
1.5×10⁵
1×10⁵
5×10⁴
0
0
5
10
15
20
Soak time (minutes)
B
Effect of Dry Time on Screw Bacterial Load
CFU
8×10⁴
6×10⁴
4×10⁴
2×10⁴
0
0
5
10
15
20
25
Dry time (minutes)
C
Bacteria Recovered from ex vivo Orthopedic Screws at Day 7
log10 (CFU/mL)
6
4
2
0
Fosfomycin
Phage
Dual
Control

Figure 5

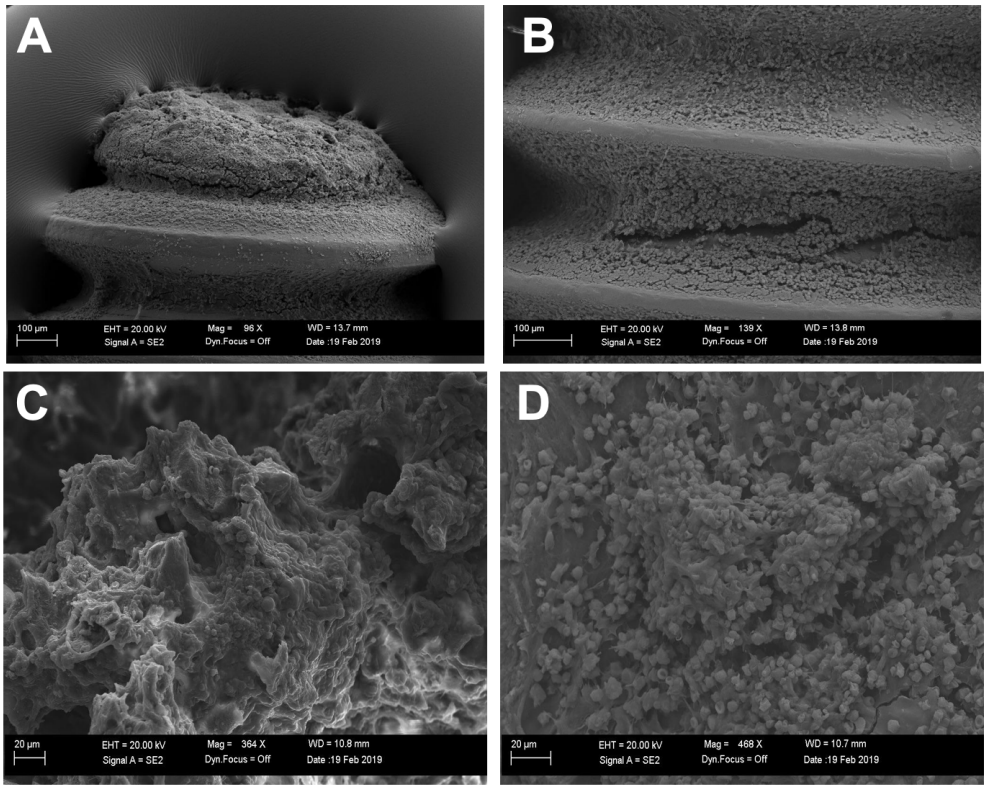
A
100 µm
EHT = 20.00 kV
Signal A = SE2
Mag = 96 X
Dyn.Focus = Off
WD = 13.7 mm
Date :19 Feb 2019
B
100 µm
EHT = 20.00 kV
Signal A = SE2
Mag = 139 X
Dyn.Focus = Off
WD = 13.8 mm
Date :19 Feb 2019
C
20 µm
EHT = 20.00 kV
Signal A = SE2
Mag = 364 X
Dyn.Focus = Off
WD = 10.8 mm
Date :19 Feb 2019
D
20 µm
EHT = 20.00 kV
Signal A = SE2
Mag = 468 X
Dyn.Focus = Off
WD = 10.7 mm
Date :19 Feb 2019

Figure 6

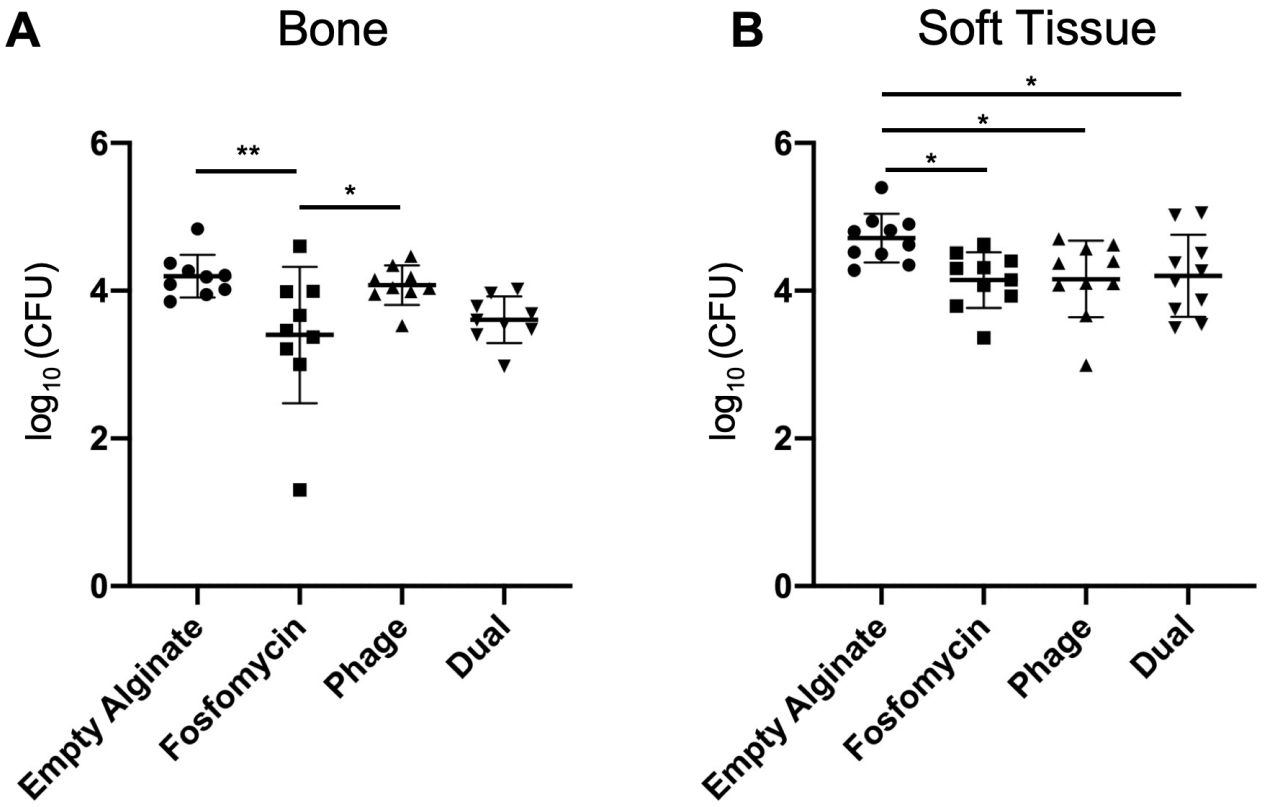

Text

Figure 7

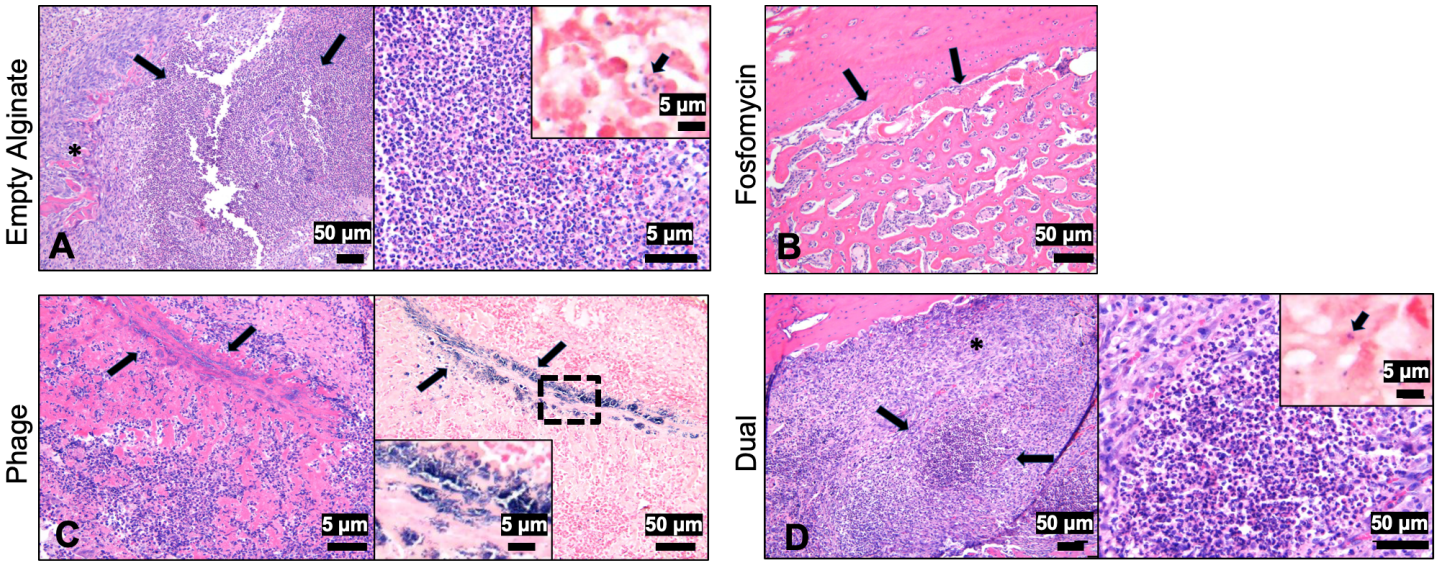
Empty Alginate
A
50 µm
5 µm
5 µm
Fosfomycin
B
50 µm
Phage
C
5 µm
5 µm
50 µm
Dual
D
50 µm
5 µm
50 µm